Geosciences Journal
Vol. 8, No. 1, p. 11 − 25, March 2004

2004-1-508
(SCI)

Geochemistry of volcanic rocks in Barton and Weaver peninsulas, King George Island, Antarctica: Implications for arc maturity and correlation with fossilized volcanic centers

Jeong Pil Yeo* — *Department of Earth Science Education, Seoul National University, Seoul 151-748, Korea*
Jong Ik Lee, Soon Do Hur — *Korea Polar Research Institute, Korea Ocean Research and Development Institute, Ansan P.O. Box 29, Seoul 425-600, Korea*
Byeon-Gak Choi — *Department of Earth Science Education, Seoul National University, Seoul 151-748, Korea*

ABSTRACT: We investigated geochemical characteristics of the Paleocene-Eocene volcanic rocks in Barton and Weaver peninsulas, King George Island, Antarctica. Volcanic rocks are predominantly tholeiitic, and show geochemical properties typical for island arc volcanism. The volcanic rocks can be subdivided into three groups based on the differences of geochemistry and regional distribution. The group 1 rocks are distributed in Weaver Peninsula and in the central part of Barton Peninsula. They show relatively mafic compositions (basalts to basaltic andesites) with the lowest level of total REEs. The group 2 rocks are widely distributed in Barton Peninsula, and show intermediate compositions (basaltic andesites to andesites) with the highest LILE/HFSE and LREE/HREE ratios. The group 3 rocks occur as intermediate dikes or plugs along the southern coast of Barton Peninsula. They generally show similar compositions to those of the group 2, but have smaller LREE/HREE ratios. The parental magma of the group 1 seems to be most depleted among three groups, whereas that of the group 2 rocks enriched in LILEs and LREEs. Predominance of tholeiite series rocks, general absence of the basement complex, and difficulty of identifying dual volcanic chains suggest that the Early Tertiary volcanism in King George Island occurred in an immature island arc without thickened continental-type crust. Geochemical correlations between volcanic rocks and fossilized volcanic vents suggest that volcanic groups can be linked with vents: the group 1 with Weaver Nunatak, and the group 2 with Three Brothers Hill, Florence Nunatak and/or Czajkowski Needle. However, the group 3 seems to be correlative with the Chottaebawi plug (the Narebski Point), or represent distinct dike swarms.

Key words: island arc volcanism, arc maturity, volcanic vent, Barton and Weaver peninsulas, King George Island

1. INTRODUCTION

King George Island (KGI) is the largest island in the South Shetland Islands which were formed in a typical island arc setting around the northern Antarctic Peninsula, and consists mainly of subalkaline volcanic and plutonic rocks of Paleocene to Eocene age (Smellie et al., 1984). Barton and Weaver peninsulas are located in the southwestern part of KGI (Fig. 1). The geology, geochemistry, and isotopic nature of volcanic rocks in KGI are documented in many previous studies (Barton, 1965; Ashcroft, 1972; Birkenmajer, 1983, 1998; Smellie et al., 1984; Tokarski, 1988; Park, 1989; Jwa et al., 1992; Lee et al., 1996; Kim et al., 2000, 2002). However, it still remains unclear what stage is responsible for the major volcanism in KGI, particularly in terms of the arc maturity (primitive or mature), and where the eruption centers are located. Some of eruption centers are preserved as nunataks, which are peaks of rock appearing above the surface of the inland ice (Figs. 1 and 2). Barton (1965) suggested several fossilized volcanic centers, which are focused along the three lines parallel to the paleo-arc of the island. However, he did not resolve precisely the eruption age of each volcanic center. For example, some alkaline volcanic centers, distributed along the southeastern coast of KGI, have been proved as the Quaternary volcanics temporally related to the opening of the Bransfield Strait (Jwa et al., 1992), and hence are not related to the major Paleocene-Eocene volcanism in KGI.

It is thus necessary to investigate the geochemical properties of volcanic rocks in KGI in order to better understand the arc maturity during major volcanism and the relationship between volcanic vents and surrounding rocks. In this study, we report new geochemical data and properties of volcanic rocks in Barton and Weaver peninsulas, and discuss the extent of arc maturity during the major volcanism. In addition, we propose several possible eruption centers based on geochemical correlations with the nunataks.

2. GENERAL GEOLOGY

The South Shetland Islands (SSIs) are the Jurassic-Quaternary magmatic island arc founded on a basement of schist, gneiss and deformed sedimentary rocks. The SSIs form a 550-km-long archipelago at the southwestern end of the Scotia Ridge, and are separated from the Antarctic Peninsula by a marginal basin (Bransfield Strait). Geophysical evidence suggests that the SSIs lie on small continental plate (Ashcroft, 1972). This micro-plate may be bounded by a back-arc spreading ridge in the Bransfield Strait to the southeast, an oceanic trench to the northwest (along which subduction has apparently ceased), and transverse faults to

*Corresponding author: jpyeo@naver.com

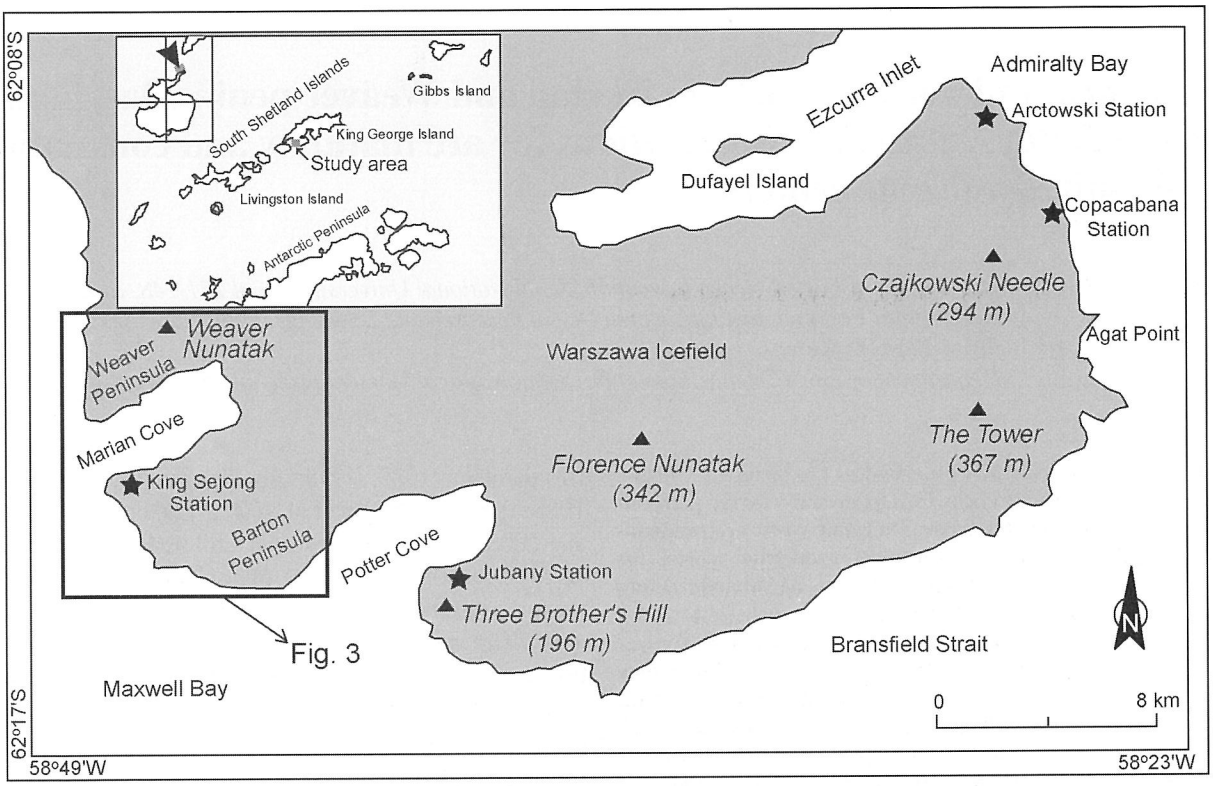

Fig. 1. A location map of representative fossilized volcanic vents, southwestern King George Island. The inset figure shows the location of the study area. Solid triangles and solid stars indicate volcanic vents and scientific stations, respectively.

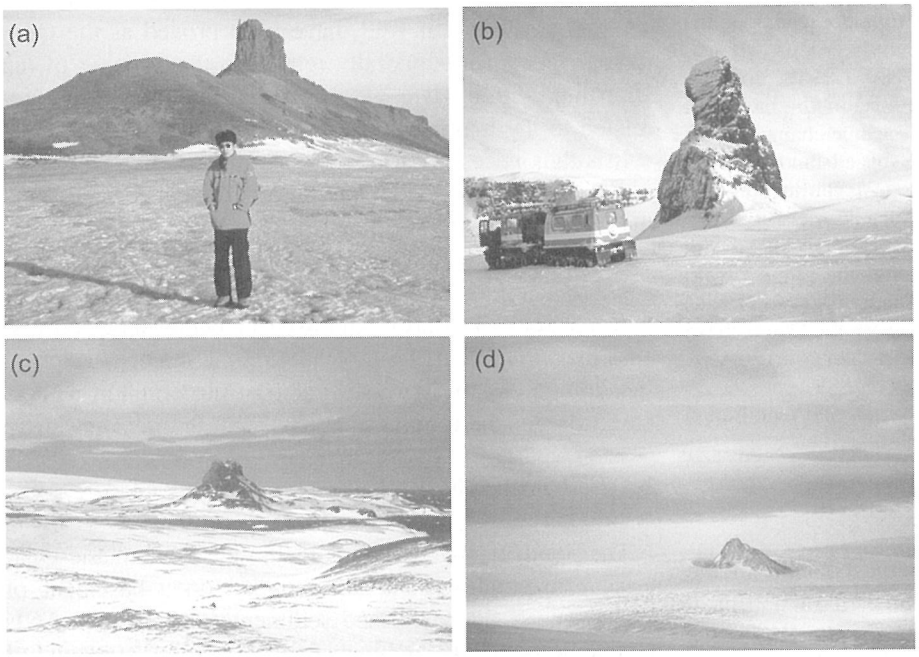

Fig. 2. Photographs of representative volcanic nunataks in southwestern King George Island. (a) The Tower, (b) Czajkowski Needle, (c) Three Brothers Hill, and (d) Florence Nunatak.

the north and south (Ashcroft, 1972; Barker and Griffiths, 1972).

An ice cap attaining 600 m in average height occupies most of the interior of KGI. This island is mostly composed of igneous rocks of pyroclastic, volcanic or plutonic origin. Contrary to the Livingston Island where the older basements commonly occur, the basement complex is not exposed on KGI. The lithostratigraphic division of KGI is slightly different among various workers. Smellie et al. (1984) suggested two formations: the lower Fildes Formation in the western part of KGI and the upper Hennequin Formation to the east. In contrast, Birkenmajer (1983,

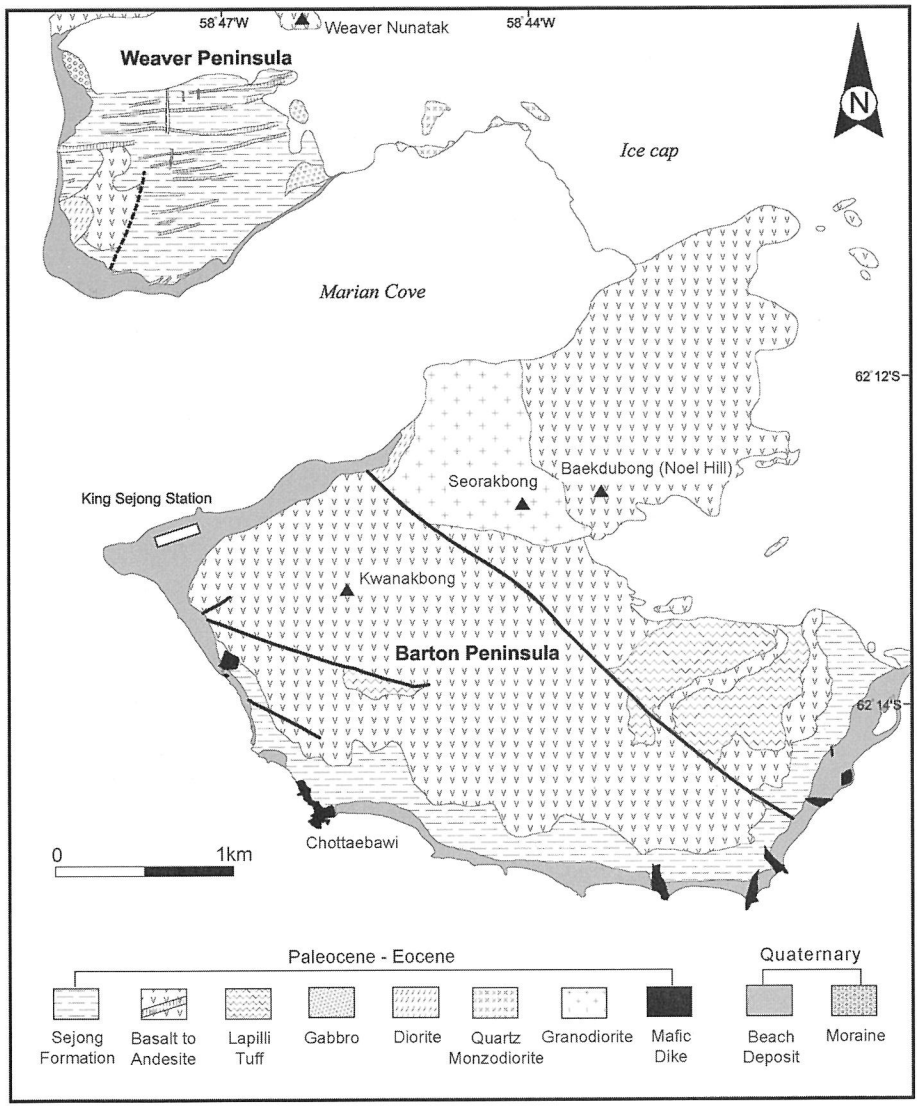

Fig. 3. Geological map of Barton and Weaver peninsulas, King George Island, Antarctica (modified from Lee et al., 2002).

1998) suggested three tectonic blocks divided by large-scale strike-slip faults: the Barton and Weaver peninsulas (Barton Horst) along the central axis of KGI, the Fildes Peninsula (Fildes Block) to the northwest and Potter Peninsula (Warszawa Block) to the southeast. He established different lithostratigraphy for each tectonic block: i.e., the Barton Horst consists mainly of Paleogene volcanic-sedimentary complex, whereas the Fildes Block, downthrown with respect to the Barton Horst, consists of Paleogene part of the Warszawa Block suite (Birkenmajer et al., 1990). In the western KGI, quartz dioritic and granodioritic plutons are observed exclusively in Barton Peninsula. Though the plutons are mainly in fault contact with the surrounding volcanic strata, the presence of volcanic enclaves suggests that the granitic rocks have apparently intruded into the volcanic strata (Jwa et al., 1992).

Most nunataks in KGI are thought to have been ancient volcanic centers (Barton, 1965). These nunataks are subalkaline basaltic andesites to andesites, and mostly show low- to medium-K and tholeiite-series geochemical properties (Lee et al., 1998). However, some nunataks, such as Three Brothers Hill, Florence Nunatak, and Czajkowski Needle are distributed along the line of hypersthene-augite andesites of Barton (1965) and commonly show transitional geochemical nature.

The lithology of Barton and Weaver peninsulas consists mainly of lavas, pyroclastics, hypabyssal and plutonic rocks (Fig. 3). The lowermost Sejong Formation (Yoo et al., 2001), formerly the Lower Volcanic Member (Davis, 1982), is distributed along the southern and southwestern coasts of Barton Peninsula, but occurs widely in Weaver Peninsula. It is largely composed of volcaniclastic sediments with a maximum thickness of about 100 m and gently dips to the south or southwest. Plant fossil leaves in fine-grained sandstones are suggestive of Late Paleocene to Eocene deposition (Chun et al., 1994).

Mafic to intermediate volcanic lavas above the Sejong Formation are widespread in Barton Peninsula. They are

mostly plagioclase-phyric or plagioclase- and clinopyroxene-phyric basalt to andesite. Several units of thick-bedded lapilli tuffs are intercalated. Although it is difficult to constrain the precise eruption ages due to alteration, most lavas seem to have erupted during Paleocene to Eocene (Pankhurst and Smellie, 1983; Smellie et al., 1984; Tokarski, 1988; Park, 1989; Kim et al., 2000; Hur et al., 2001; Willan and Armstrong, 2002).

Moderate- to small-size plugs and mafic dikes have intruded the Sejong Formation along the southern coast of Barton Peninsula. In Weaver Peninsula, east-trending mafic dikes are common and cut by north-trending dikes.

A granodioritic stock with minor fine-grained diorite occurs in the northern Barton Peninsula. Park (1989) reported whole-rock K–Ar ages of 42 to 45 Ma, and comparable K–Ar biotite ages of 41.9± 0.9 Ma and 41.2± 0.9 Ma are also reported by Lee et al. (1996). Kim et al. (2000) reported $^{40}Ar/^{39}Ar$ age of 48.4± 0.5 Ma for fine-grained diorite. This pluton is thus interpreted to have intruded in middle Eocene. Small stocks of medium to fine-grained gabbro, diorite, and quartz monzodiorite have intruded the Sejong Formation and the overlying basaltic lava succession in Weaver Peninsula.

3. OCCURRENCE AND PETROGRAPHY

3.1. Volcanic Rocks

3.1.1. Lavas

Mafic to intermediate volcanic lavas (basaltic andesite to andesite) overlying the Sejong Formation are widespread in Barton Peninsula. Small volume of plagioclase-phyric basaltic andesite lava, overlying or fault-contacted with the Sejong Formation, is present in the southwestern part of Weaver Peninsula. These lavas mostly contain euhedral to subhedral phenocrysts of either plagioclase only or plagioclase and clinopyroxene. Modal contents of phenocrysts are mostly about 10–20% and less than 40%. Plagioclase phenocrysts (labradorite to andesine) commonly show normal zoning. Some mafic lavas are glomeroporphyritic and subophitic.

3.1.2. Dikes

Several mafic plugs and dikes trending toward north or northwest have intruded the Sejong Formation along the southwestern coast of Barton Peninsula. They are generally plagioclase-phyric or massive basaltic andesites, and commonly show microscopic flow structures. Moderate-size volcanic plug around the Chottaebawi (a penguin rookery site) has distinct joint patterns, and is proposed as a volcanic vent by Tokarski (1988) and Birkenmajer (1998). In Weaver Peninsula, on the other hand, east-trending basaltic dikes are abundant. They are plagioclase-phyric or plagioclase- and clinopyroxene-phyric basalts of 1 to 5 m in width, and are generally cut by north-trending dikes of similar compositions. Dikes of Weaver Peninsula are similar to mafic lavas in northwestern part of Barton Peninsula in petrographic characteristics.

3.2. Plutonic Rocks

The plutonic rocks in Barton and Weaver peninsulas show a wide range of modal composition. According to the classification scheme of IUGS (1973), they are classified into gabbro, diorite, quartz monzodiorite, granodiorite, and granite. Granodiorite forms a stock in association with minor fine-grained diorite in northern Barton Peninsula. Although granodiorite and diorite show a transitional contact, compositional variation is suggestive of different intrusive episodes (Lee et al., 1996). Mafic to intermediate plutonic rocks such as gabbro, diorite, and quartz monzodiorite occur as isolated, small stocks in Weaver Peninsula.

4. GEOCHEMISTRY

4.1. Analytical Procedures

Samples were broken into 1-2 centimeter sized chips, and then altered parts were removed. The chips were crushed into coarse grains in a tungsten carbide crusher and finally ground into fine powder by automatic agate ball mill. The prepared powders were analyzed for major, trace and rare earth elements.

Major element compositions were determined by an X-ray fluorescence spectrometry (XRF, Philips PW1480) using fused glass beads at Korea Polar Research Institute, Korea Ocean Research and Development Institute (KORDI), following the procedure outlined by Lee (1994). Trace and rare earth elements were analyzed by an inductively coupled plasma mass spectrometry (ICP-MS, PerkinElmer, Elan 6100) at KORDI. The accuracy of the analysis is better than 3% for major elements (Lee, 1994), and 5% for most trace and rare earth elements. The analytical results are summarized in Table 1.

4.2. Major Element Chemistry

Major element compositions for volcanic rocks are given in Table 1, and those for plutonic rocks are referred to Lee et al. (1996). The data of plutonic rocks are plotted together in the following diagrams because there are fundamental geochemical differences between plutonic and volcanic rocks. The subdivision of plutonic rocks is based on the modal classification (Lee et al., 1996), whereas that of volcanic rocks on geochemical properties described below.

The SiO_2 contents of plutonic rocks widely vary from 48 to 71 wt% defining a relatively simple trend in total alkalis vs. silica diagram (Fig. 4), whereas those of volcanic rocks range from 48 to 60 wt% with variable alkali contents. Both

Table 1. Major, trace and rare earth element compositions of volcanic rocks.

Rock Type	B	B	B	B	B	B	B	B	B	BA	BA	BA	BA
Sample No.	0705-3	2908	1129	1507-2	1007	1507-3	0513	1110	1002	1001	2910	1216	2906
Group	1	1	1	1	1	1	1	1	1	1	1	1	1
SiO_2	47.46	46.04	49.79	50.87	51.39	50.60	49.00	50.51	50.18	49.41	49.79	51.57	50.04
TiO_2	0.47	0.68	0.74	0.70	0.83	0.70	0.61	0.72	0.58	0.61	0.73	0.73	0.69
Al_2O_3	21.23	17.94	19.42	22.47	20.51	20.82	18.44	19.02	20.80	19.33	18.10	18.90	17.31
FeO*	8.40	9.21	8.82	7.70	8.50	8.06	8.25	9.23	7.19	7.49	8.74	8.38	9.07
MnO	0.16	0.14	0.16	0.19	0.16	0.19	0.11	0.15	0.11	0.12	0.14	0.18	0.18
MgO	6.77	6.04	5.50	3.89	5.22	4.44	3.70	5.22	4.80	4.65	4.52	4.76	3.62
CaO	14.53	10.51	10.96	11.43	8.90	9.37	12.55	9.81	9.77	8.38	8.51	8.26	7.68
Na_2O	0.99	1.86	2.76	2.31	3.93	3.43	2.05	2.92	2.93	3.41	3.08	3.37	2.76
K_2O	0.06	0.09	0.28	0.33	0.53	0.41	0.16	0.21	0.54	0.37	0.25	0.52	2.16
P_2O_5	0.07	0.13	0.13	0.12	0.14	0.11	0.11	0.13	0.13	0.14	0.14	0.22	0.16
LOI	0.34	7.39	1.25	0.38	0.24	1.46	4.50	2.30	3.17	6.01	5.57	3.12	6.55
Total	100.48	100.03	99.82	100.39	100.34	99.59	99.49	100.21	100.20	99.92	99.57	100.01	100.22
Trace and rare earth elements (in ppm)													
Sc	20.9	31.3	32.9	20.5	22.6	19.3	30.9	30.2	21.3	24.0	26.2	22.8	33.9
V	168.3	243.3	245.5	218.5	249.9	210.3	196.9	233.0	178.0	185.7	217.8	189.3	286.8
Cr	19.0	22.0	27.3	5.1	9.2	8.6	39.8	11.1	18.4	19.0	12.0	16.3	3.5
Co	31.6	37.3	32.3	16.5	22.9	19.4	36.0	32.0	25.1	26.9	26.3	24.8	36.3
Ni	26.8	22.1	25.0	11.9	9.6	10.6	34.9	15.2	17.3	15.6	10.1	197.5	6.0
Cu	50.2	122.7	67.4	90.8	90.4	107.7	103.3	195.2	57.4	95.8	115.1	106.8	153.8
Zn	38.5	74.4	68.1	42.3	63.8	50.3	67.9	70.0	47.9	62.2	64.4	90.2	132.9
Ga	12.9	19.4	19.0	14.5	15.1	15.1	19.0	19.3	18.8	18.7	19.0	18.6	28.5
Mo	0.2	0.7	0.8	0.2	0.2	0.1	0.5	0.6	0.6	0.5	0.7	0.7	1.2
Sn	0.4	1.9	0.7	0.5	0.7	0.6	0.5	0.5	1.9	1.9	2.0	0.6	2.7
Cs	0.6	0.6	0.1	2.8	1.5	3.9	0.6	0.0	0.3	0.7	0.5	0.4	3.6
Ba	28.5	52.9	112.1	79.1	95.9	79.0	92.7	113.0	127.5	103.2	128.8	180.9	283.6
Rb	0.4	1.3	2.6	3.9	9.2	7.5	1.2	1.0	5.4	5.0	4.1	5.3	60.7
Sr	414.6	523.3	544.5	556.8	717.0	721.5	575.2	611.5	609.8	684.4	730.2	525.4	771.9
Y	6.5	11.8	13.2	8.2	11.1	9.3	11.2	12.1	9.3	10.9	12.5	13.1	20.3
Zr	28.8	40.5	37.3	36.4	50.5	51.6	52.3	38.8	26.3	46.4	58.3	22.5	84.5
Nb	0.5	1.0	1.2	0.7	1.3	1.2	1.5	0.9	1.0	1.2	1.5	1.5	1.8
Hf	1.0	1.2	1.1	1.4	1.8	1.8	1.4	1.1	0.8	1.3	1.6	0.7	2.3
Ta	0.0	0.1	0.2	0.0	0.1	0.1	0.2	0.1	0.1	0.2	0.2	0.1	0.2
W	12.5	0.1	0.1	4.6	16.7	2.8	0.1	0.1	0.1	0.1	0.1	0.1	0.2
Pb	3.1	2.9	3.0	2.5	6.1	2.5	13.9	3.5	3.2	3.4	4.2	3.3	7.2
Th	1.1	0.8	0.6	1.1	1.1	1.2	0.9	0.7	0.7	0.8	2.2	0.6	4.0
U	0.2	0.2	0.2	0.3	0.3	0.3	0.3	0.3	0.3	0.3	0.6	0.2	0.9
La	5.6	5.1	5.8	5.9	7.0	6.4	7.8	5.2	5.5	6.4	11.1	6.6	20.0
Ce	11.3	12.7	14.5	13.6	16.1	14.6	18.4	12.7	13.3	15.3	25.1	16.4	43.6
Pr	1.6	1.8	2.0	2.0	2.4	2.2	2.5	1.8	1.8	2.1	3.1	2.3	5.4
Nd	7.2	9.0	10.2	9.5	11.6	10.1	11.7	9.0	9.0	10.0	14.1	11.2	23.6
Sm	1.7	2.4	2.7	2.4	3.0	2.6	2.9	2.4	2.3	2.5	3.2	2.8	5.3
Eu	0.6	0.8	1.0	0.9	1.1	0.9	0.9	0.9	0.8	0.9	1.0	1.0	1.7
Gd	1.8	2.3	2.4	2.5	3.1	2.6	2.4	2.3	2.0	2.2	2.6	2.6	4.4
Tb	0.3	0.4	0.4	0.4	0.5	0.4	0.4	0.4	0.3	0.3	0.4	0.4	0.7
Dy	1.5	2.2	2.4	2.1	2.6	2.2	2.2	2.3	1.9	2.1	2.4	2.5	4.0
Ho	0.3	0.5	0.5	0.4	0.5	0.4	0.5	0.5	0.4	0.4	0.5	0.5	0.8
Er	0.8	1.3	1.4	1.1	1.5	1.2	1.2	1.3	1.0	1.2	1.4	1.4	2.2
Tm	0.1	0.2	0.2	0.2	0.2	0.2	0.2	0.2	0.1	0.2	0.2	0.2	0.3
Yb	0.7	1.1	1.2	1.0	1.3	1.1	1.0	1.2	0.9	1.0	1.2	1.2	1.9
Lu	0.1	0.1	0.2	0.1	0.2	0.2	0.1	0.2	0.1	0.1	0.2	0.2	0.3

Abbreviations: B, basalt; BA, basaltic andesite; A, andesite.
*total Fe as FeO, LOI: loss on ignition

Table 1. (Continued).

Rock Type	BA	BA	BA	BA	BA	BA	BA	BA	BA	BA	BA	BA	BA	BA	BA
Sample No.	2909	1215	1505	1503	1003	1213	1103	1002	1502	0705-1	1817	0930	0906	0201	0911
Group	1	1	1	1	1	1	1	1	1	1	2	2	2	2	2
SiO_2	51.56	53.02	54.22	54.23	52.41	53.42	54.20	55.22	55.69	56.06	52.88	53.40	53.10	53.14	53.67
TiO_2	0.94	0.76	0.94	0.75	0.68	0.73	0.76	0.61	0.68	0.99	0.78	0.75	0.75	0.82	0.70
Al_2O_3	16.78	18.74	17.73	19.05	18.02	18.46	18.75	19.50	19.08	18.94	18.03	18.03	17.06	18.24	17.91
FeO*	10.35	8.88	9.46	8.87	7.82	8.63	8.64	6.90	6.99	7.85	8.36	8.69	8.11	8.97	7.95
MnO	0.18	0.16	0.20	0.16	0.13	0.16	0.14	0.17	0.14	0.16	0.15	0.13	0.12	0.12	0.16
MgO	4.09	4.41	4.18	4.10	3.96	4.31	4.41	4.12	4.05	3.15	4.55	4.38	4.76	3.37	4.17
CaO	8.04	8.43	8.21	8.97	8.42	8.20	8.42	8.59	9.51	7.12	8.15	8.25	8.13	7.22	8.26
Na_2O	3.87	3.32	4.34	3.10	3.32	3.17	3.26	3.83	3.07	3.88	3.35	3.25	2.74	3.39	2.79
K_2O	0.15	0.67	0.24	0.21	1.30	0.45	0.26	0.28	0.19	1.66	1.06	1.13	1.52	0.97	0.22
P_2O_5	0.18	0.20	0.19	0.17	0.17	0.20	0.19	0.13	0.17	0.31	0.26	0.22	0.24	0.27	0.20
LOI	3.82	1.30	0.39	0.35	3.56	2.17	0.82	0.76	0.42	0.36	1.95	1.46	3.38	3.78	3.86
Total	99.96	99.89	100.08	99.96	99.79	99.90	99.85	100.11	99.98	100.46	99.51	99.69	99.92	100.29	99.90
Trace and rare earth elements (in ppm)															
Sc	37.3	23.9	26.2	20.3	24.9	24.0	25.1	16.0	17.0	19.1	28.4	25.3	24.8	27.5	24.7
V	312.2	193.5	292.5	204.8	194.5	194.5	193.2	139.1	211.6	201.0	220.7	194.5	176.0	222.1	183.6
Cr	0.2	18.0	4.3	8.0	13.9	15.6	20.0	18.3	20.7	3.6	22.4	20.3	11.9	14.1	7.7
Co	28.7	28.1	19.2	20.6	24.7	25.8	27.0	26.4	18.4	12.8	27.0	26.6	20.7	24.0	24.6
Ni	2.6	12.9	15.6	5.9	10.6	9.1	13.2	13.1	13.5	10.4	16.3	16.7	7.0	13.8	64.3
Cu	180.2	104.0	133.9	86.0	100.6	103.9	178.8	52.9	88.3	111.9	115.7	97.8	144.6	160.1	77.4
Zn	92.4	84.0	83.7	65.5	75.9	63.0	77.0	55.3	62.0	70.4	82.3	81.4	77.3	82.4	84.4
Ga	22.0	19.6	16.3	16.2	19.9	20.7	19.9	14.9	16.8	15.8	20.4	20.8	19.6	21.2	19.7
Mo	0.9	0.8	0.5	0.6	1.4	1.1	0.8	0.8	0.8	0.2	1.8	2.0	1.1	1.2	0.6
Sn	2.0	0.7	1.1	1.0	2.3	0.8	0.7	0.8	0.9	0.8	0.9	1.1	1.2	1.2	0.9
Cs	1.2	0.6	0.6	0.4	0.4	0.3	0.2	0.1	0.3	2.6	0.2	0.2	1.3	1.0	0.1
Ba	93.9	182.4	111.3	120.6	265.7	149.1	162.5	134.5	142.8	220.9	254.5	257.8	600.3	466.6	178.3
Rb	3.1	6.4	1.9	1.8	17.1	6.0	2.0	2.5	0.7	22.4	14.4	13.3	49.1	12.2	1.1
Sr	823.4	568.0	593.7	549.9	750.6	544.9	606.0	501.8	639.0	440.3	602.4	645.6	535.6	793.9	588.6
Y	17.0	14.3	12.7	12.2	14.9	14.7	14.2	9.2	9.1	14.4	18.5	19.6	22.4	19.2	17.3
Zr	65.1	45.2	51.6	59.7	88.5	42.3	52.2	43.5	76.7	67.2	105.8	135.3	153.4	128.4	109.7
Nb	1.8	1.6	1.0	1.3	2.1	1.7	1.6	1.8	2.1	1.5	2.2	2.9	3.2	3.0	3.0
Hf	1.8	1.3	2.0	2.0	2.5	1.2	1.5	1.1	2.7	2.4	2.8	3.4	4.2	3.3	2.7
Ta	0.4	0.1	0.1	0.1	0.2	0.2	0.2	0.1	0.1	0.1	0.2	0.2	0.2	0.2	0.6
W	0.2	0.1	9.2	33.2	0.2	0.1	0.1	82.0	2.9	5.5	0.2	0.2	0.2	0.2	0.2
Pb	3.6	2.6	2.9	3.3	13.3	4.8	3.8	3.1	7.3	4.4	5.8	5.4	6.0	5.9	5.4
Th	1.2	0.8	1.3	3.2	4.0	0.7	0.7	0.8	2.1	1.8	2.3	2.7	3.6	2.5	2.4
U	0.4	0.3	0.4	0.6	1.3	0.3	0.2	0.2	0.7	0.4	0.9	0.8	1.4	0.9	0.7
La	8.9	7.9	8.8	13.3	14.0	8.4	7.5	6.0	7.7	12.0	14.7	14.1	19.8	16.7	12.0
Ce	21.6	19.0	20.0	27.0	31.6	19.9	18.0	13.1	17.5	26.5	34.8	33.6	47.0	39.6	28.5
Pr	3.0	2.6	3.1	3.7	3.9	2.6	2.5	1.9	2.5	3.9	4.6	4.2	5.9	5.0	3.7
Nd	14.5	12.5	14.5	15.9	17.8	12.6	11.9	8.8	11.0	17.9	21.5	19.5	27.1	23.2	17.1
Sm	3.8	3.1	3.8	3.6	3.9	3.1	3.0	2.2	2.7	4.3	5.0	4.5	6.0	5.3	3.9
Eu	1.3	1.1	1.4	1.2	1.2	1.1	1.0	0.9	0.9	1.6	1.4	1.3	1.5	1.4	1.1
Gd	3.4	2.7	3.8	3.6	3.2	2.7	2.7	2.4	2.7	4.3	4.1	3.8	5.0	4.3	3.4
Tb	0.5	0.4	0.5	0.5	0.5	0.4	0.4	0.4	0.4	0.6	0.6	0.6	0.7	0.6	0.5
Dy	3.3	2.6	3.2	2.8	3.0	2.6	2.6	2.2	2.3	3.5	3.7	3.5	4.5	3.9	3.2
Ho	0.7	0.5	0.6	0.5	0.6	0.5	0.6	0.4	0.4	0.6	0.8	0.7	0.9	0.8	0.7
Er	1.8	1.5	1.7	1.5	1.7	1.5	1.5	1.2	1.3	1.9	2.0	2.0	2.5	2.1	1.8
Tm	0.2	0.2	0.2	0.2	0.2	0.2	0.2	0.2	0.2	0.3	0.3	0.3	0.3	0.3	0.2
Yb	1.6	1.4	1.6	1.4	1.4	1.3	1.4	1.1	1.3	1.8	1.7	1.7	2.1	1.7	1.6
Lu	0.2	0.2	0.2	0.2	0.2	0.2	0.2	0.2	0.2	0.3	0.2	0.3	0.3	0.3	0.2

Table 1. (Continued).

Rock Type	BA	BA	BA	BA	A	A	A	A	A	BA	BA	BA	BA	BA	A
Sample No.	0926	0929	0605	2512	2102	0205	1112	2322	0902	1105	1105-1	1105-2	0107	0108	0601
Group	2	2	2	2	2	2	2	2	2	3	3	3	3	3	3
SiO_2	54.55	54.84	54.25	54.90	55.37	55.06	57.22	57.65	58.60	56.70	54.76	55.89	55.18	55.90	56.46
TiO_2	0.73	0.70	0.83	0.78	0.76	0.82	1.04	1.03	0.85	1.44	1.39	1.40	1.12	1.08	0.91
Al_2O_3	17.72	17.97	17.60	17.64	14.48	17.21	15.84	15.77	16.73	16.10	15.67	15.84	18.45	17.68	17.99
FeO*	7.71	7.68	7.47	7.96	7.94	7.33	8.21	8.33	6.67	9.96	9.53	9.65	8.19	7.93	7.33
MnO	0.14	0.15	0.13	0.13	0.13	0.12	0.15	0.14	0.12	0.19	0.17	0.18	0.15	0.21	0.16
MgO	4.29	3.46	2.65	3.36	4.07	2.74	3.19	3.00	2.19	3.48	3.93	3.95	3.47	3.11	3.07
CaO	8.31	8.24	8.26	6.96	8.03	6.25	5.27	5.17	5.25	6.92	7.51	6.80	6.74	6.53	7.26
Na_2O	2.76	2.77	3.26	3.38	2.81	3.41	3.45	3.96	3.68	3.97	3.08	3.20	4.40	4.60	3.95
K_2O	1.16	1.06	0.74	1.13	1.75	1.75	2.73	2.29	2.49	1.96	1.77	1.65	0.37	1.11	1.21
P_2O_5	0.21	0.19	0.27	0.25	0.21	0.31	0.42	0.41	0.37	0.46	0.43	0.44	0.27	0.32	0.27
LOI	2.76	3.11	4.26	3.29	4.26	4.67	2.36	2.27	3.04	0.21	1.59	0.72	1.62	2.01	1.48
Total	100.31	100.17	99.70	99.78	99.79	99.66	99.87	100.02	99.98	101.37	99.81	99.72	99.95	100.48	100.09
Trace and rare earth elements (in ppm)															
Sc	23.6	24.3	26.1	25.4	25.3	23.2	26.6	24.9	29.1	26.8	28.6	23.9	24.1	24.0	22.8
V	185.2	182.0	195.1	199.7	185.9	170.1	216.0	185.8	207.2	255.0	261.2	233.9	252.2	135.1	195.2
Cr	18.1	12.5	10.3	10.0	15.2	10.7	0.4	1.5	31.2	8.5	10.4	9.2	1.2	0.8	4.3
Co	24.7	26.5	21.4	22.2	25.6	20.2	18.2	17.6	28.6	23.3	16.6	16.1	17.9	14.2	12.5
Ni	62.1	12.2	8.1	6.9	12.0	8.1	2.4	3.5	15.7	6.7	7.6	7.3	3.7	1.4	12.0
Cu	129.2	133.5	126.2	123.9	159.8	87.9	204.0	185.9	108.5	133.9	305.2	226.5	155.3	53.3	108.9
Zn	90.5	82.8	79.2	75.9	76.8	81.1	100.8	88.1	85.1	77.3	75.0	70.1	82.1	69.8	59.3
Ga	19.5	19.9	21.0	20.6	19.9	20.3	21.2	19.4	19.7	14.7	14.0	13.1	17.4	15.3	15.2
Mo	1.8	1.6	1.2	1.2	1.5	1.1	2.5	2.1	1.0	1.2	1.1	1.2	1.3	0.7	0.8
Sn	1.1	1.2	1.1	1.2	1.2	1.5	1.6	1.6	1.0	1.6	1.5	1.5	1.3	1.6	1.2
Cs	0.1	0.1	0.8	0.9	1.1	1.8	1.0	0.4	0.3	0.3	0.3	0.4	2.6	0.7	0.6
Ba	432.6	333.0	299.3	350.5	301.7	402.4	450.3	446.6	336.8	350.0	277.3	304.1	194.9	288.5	407.0
Rb	11.5	10.2	8.7	14.6	26.5	34.8	44.1	42.9	23.3	20.3	20.6	21.5	4.2	11.9	13.0
Sr	571.8	541.3	691.6	768.2	558.4	822.7	521.4	450.2	621.1	397.1	359.0	385.4	594.7	427.2	483.6
Y	18.4	20.6	21.4	20.7	19.3	25.4	31.9	30.0	19.3	22.9	23.7	21.9	19.1	20.3	18.1
Zr	131.1	149.3	131.6	137.3	89.9	187.3	214.7	204.7	119.7	160.2	151.0	146.4	100.3	107.1	133.7
Nb	2.9	3.4	3.1	2.8	4.0	4.2	4.4	4.3	3.0	5.1	5.0	4.8	4.2	3.8	2.7
Hf	3.3	3.7	3.5	3.7	2.3	4.8	5.4	5.4	3.2	4.9	4.8	4.9	3.5	3.6	4.5
Ta	0.3	0.3	0.2	0.2	0.7	0.3	0.3	0.3	0.2	0.3	0.3	0.3	0.3	0.2	0.2
W	0.2	0.2	0.2	0.2	0.4	0.2	0.3	0.4	0.7	42.8	1.1	0.9	24.6	18.6	8.9
Pb	7.3	6.9	9.1	7.5	6.2	6.1	6.9	7.7	5.1	6.1	5.2	5.4	5.1	5.4	4.2
Th	2.8	3.2	2.7	2.9	3.5	3.9	4.2	4.0	2.8	3.8	4.1	4.0	2.4	2.5	3.0
U	0.8	1.0	0.9	1.1	1.2	1.4	1.4	1.3	1.0	0.9	0.9	0.9	0.6	0.5	0.7
La	15.6	17.0	17.9	18.0	16.6	24.2	27.7	26.3	17.3	18.3	19.9	19.8	13.8	14.8	17.8
Ce	37.1	40.0	42.2	42.1	39.1	57.0	65.4	61.7	40.6	39.5	42.9	42.8	29.8	31.3	40.0
Pr	4.6	4.9	5.4	5.4	4.9	7.1	8.2	7.8	5.1	5.7	6.2	6.1	4.3	4.5	5.6
Nd	21.1	22.4	25.0	24.8	22.5	32.5	37.7	35.8	23.7	25.5	27.4	27.1	19.7	20.6	24.7
Sm	4.8	5.1	5.7	5.5	5.1	7.2	8.4	7.9	5.2	6.0	6.5	6.4	4.8	5.0	5.7
Eu	1.3	1.3	1.5	1.4	1.3	1.7	2.0	1.8	1.4	1.7	1.8	1.8	1.6	1.7	1.7
Gd	3.9	4.2	4.6	4.6	4.1	5.7	6.8	6.6	4.3	6.1	6.6	6.4	4.9	5.2	5.5
Tb	0.6	0.6	0.7	0.7	0.6	0.8	1.0	1.0	0.7	0.9	1.0	0.9	0.7	0.8	0.8
Dy	3.5	3.8	4.1	4.1	3.7	5.0	6.0	5.9	3.9	5.3	5.6	5.4	4.4	4.5	4.2
Ho	0.7	0.8	0.8	0.8	0.8	1.0	1.2	1.2	0.8	1.0	1.0	1.0	0.8	0.8	0.8
Er	1.9	2.1	2.2	2.2	2.0	2.7	3.3	3.2	2.1	2.9	3.0	3.0	2.5	2.6	2.2
Tm	0.3	0.3	0.3	0.3	0.3	0.3	0.4	0.4	0.3	0.4	0.4	0.4	0.3	0.4	0.3
Yb	1.6	1.8	1.9	1.9	1.7	2.2	2.7	2.6	1.7	2.7	2.8	2.7	2.3	2.4	2.0
Lu	0.3	0.3	0.3	0.3	0.2	0.3	0.4	0.4	0.3	0.4	0.4	0.4	0.3	0.3	0.3

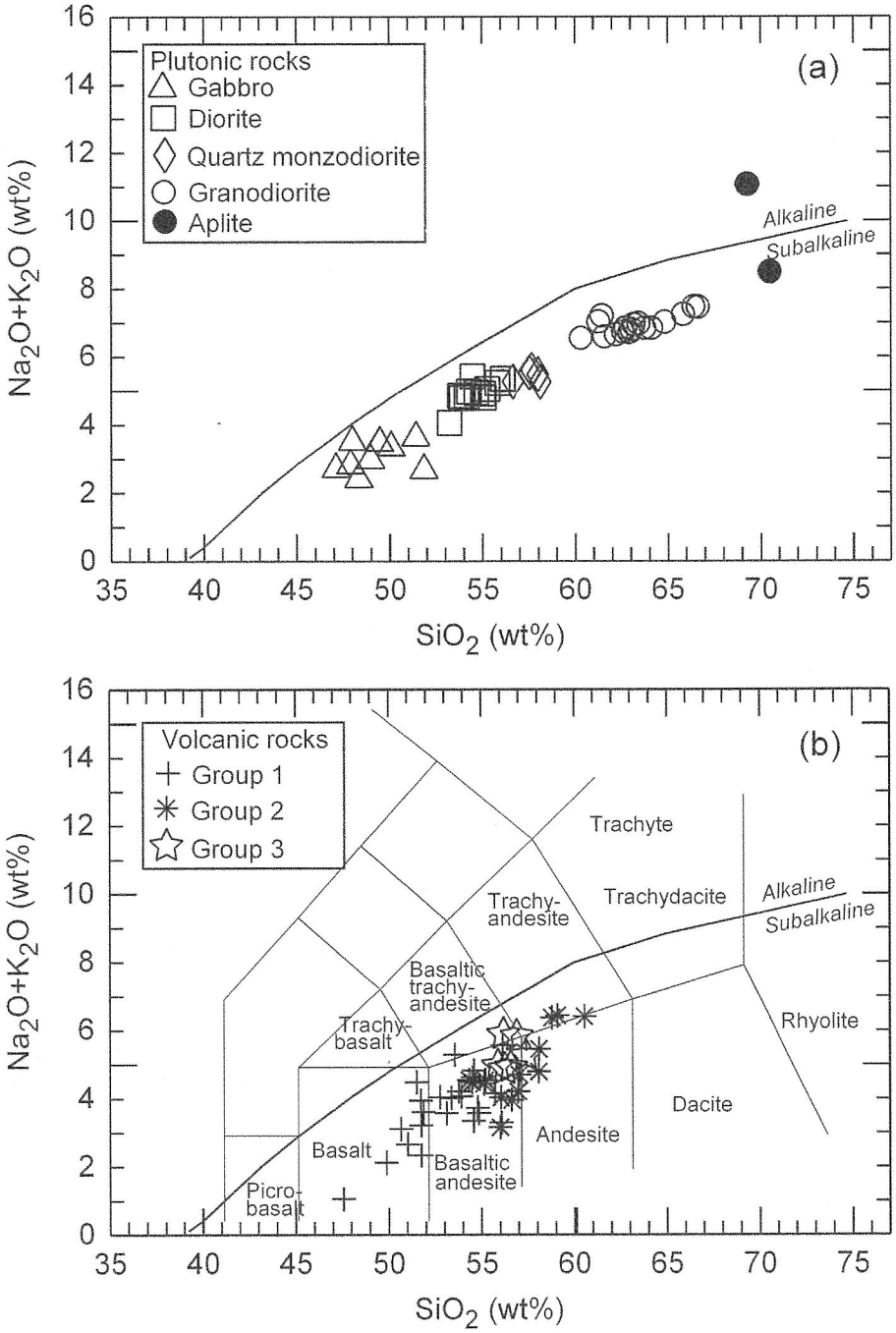

Fig. 4. Chemical classification of (a) plutonic and (b) volcanic rocks using the total alkalis versus silica diagram of Le Maitre et al. (1989). The boundary between alkaline and subalkaline series is from Irvine and Baragar (1971). Volcanic rocks are subdivided into three groups, as explained in text.

rock types belong to subalkaline series, and the majority of compositional data overlap, except for the absence of felsic volcanic rocks.

Figure 5 shows the FeO*/MgO versus SiO_2 relations (so called Miyashiro diagram) of volcanic and plutonic rocks. Miyashiro (1974) suggested several geochemical schemes for dividing subalkaline rocks into tholeiitic (TH) and calc-alkaline (CA) series in active arc environments because the proportion of TH and CA series basically depends on the arc maturity. Among these schemes, he suggested that the FeO*/MgO versus SiO_2 relation is most reliable. In practice, however, because the CA series shows higher rates of the SiO_2 increase with increasing FeO*/MgO, the slope of a rock series in Figure 5 is more important than the empirical division line. Thus the CA and TH series are defined as having steeper and gentler slopes, respectively. The plutonic rocks in Barton and Weaver peninsulas with a steep slope in Figure 5 are interpreted as the CA series, although gabbros and diorites are plotted in the field of TH series. On the contrary, the majority of volcanic rocks are plotted in the field of TH series with a slope similar to that of the empirical division line. Hence we interpret that the volcanic rocks

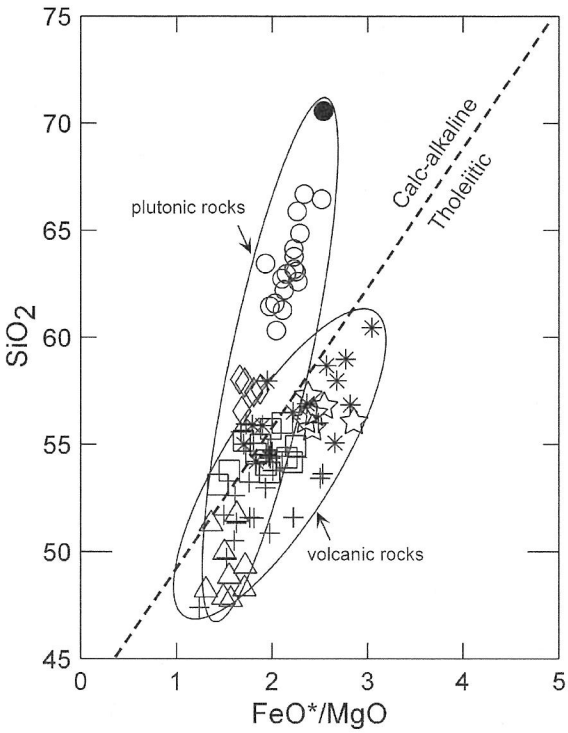

Fig. 5. FeO*/MgO versus SiO_2 diagram for discriminating calc-alkaline and tholeiitic rock series. The symbols are the same as in Fig. 4.

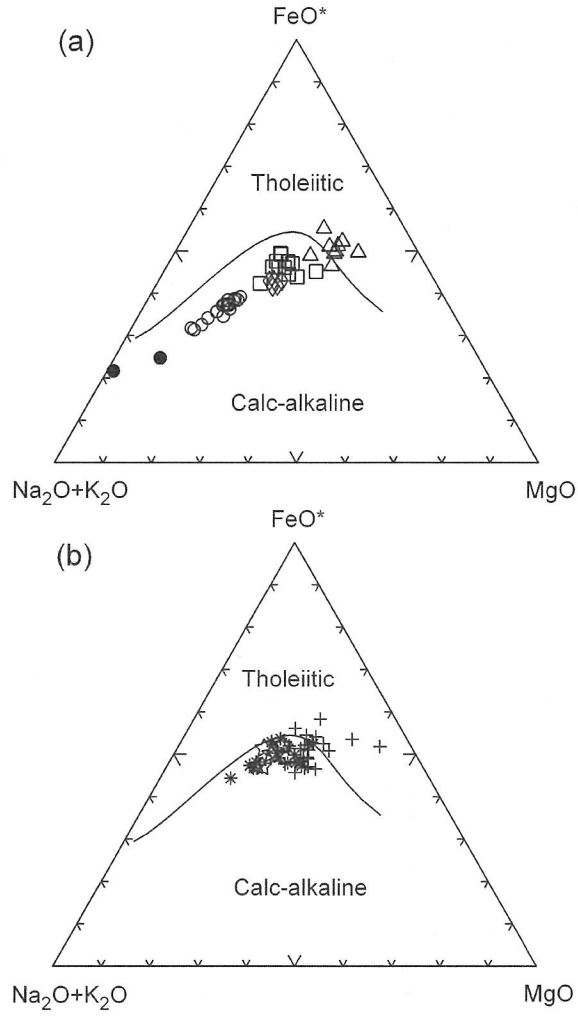

Fig. 6. The AFM diagrams of (a) plutonic and (b) volcanic rocks. The boundary between tholeiite and calc-alkaline series is from Irvine and Baragar (1971). The symbols are the same as in Fig. 4.

belong to the TH series, in contrast to most of previous studies (e.g., Birkenmajer, 1983, 1998; Smellie et al., 1984) favoring the CA series. Jwa and Lee (1992) also suggested that the volcanic rocks of Fildes Peninsula in the westernmost KGI show, as a whole, tholeiitic nature. Thus we interpret that the majority of volcanic rocks in the western KGI were originated from tholeiitic parental magmas. The implication of this interpretation for understanding the arc maturity will be discussed in the following section.

The AFM diagram is commonly used for the discrimination between CA and TH rock series, and can give us additional information (Fig. 6). The plutonic rocks differentiate from gabbro to aplitic granite without significant enrichment of total Fe (FeO*), and follow a typical CA series trend (Fig. 6a). However, the differentiation trend of volcanic rocks is not easily defined (Fig. 6b). They do not show the enrichment of alkali component and the increase of FeO*/MgO ratios. This feature is common to the TH series lacking in differentiated felsic member. Osborn (1962) explained chemical differences between the CA and TH series by the variation in oxygen pressure conditions: i.e., as magnetite is unstable under low oxygen pressure condition, the melt is gradually enriched in the Fe component and produces tholeiitic rocks. Differences between CA and TH rock series are also attributed to variable H_2O contents of primary magmas (Sakuyama, 1979; Tatsumi and Eggins, 1995). Primary magma of tholeiitic rocks seems to be derived from a dry condition in the trench side of an arc environment.

Variation diagrams of plutonic rocks show simple fractionation trends governed by ferromagnesian minerals and calcic plagioclase, except for some samples with high modal contents of plagioclase (Fig. 7). The Al_2O_3, FeO* (total Fe) and CaO contents progressively decrease with decreasing MgO content. The Na_2O and P_2O_5 contents increase from mafic to intermediate compositions, and then decrease toward felsic compositions. This inflection is attributed to the fractionation of sodic plagioclase and apatite. The SiO_2 content progressively increases with decreasing MgO content, but below about 3 wt% MgO, it increases more significantly. Abrupt increase in the SiO_2 content is likely to indicate the fractionation of Fe-Ti oxides and apatite. These variation trends suggest that the plutonic rocks were originated from an identical parental magma, though they form separate, isolated stocks. The relatively well-

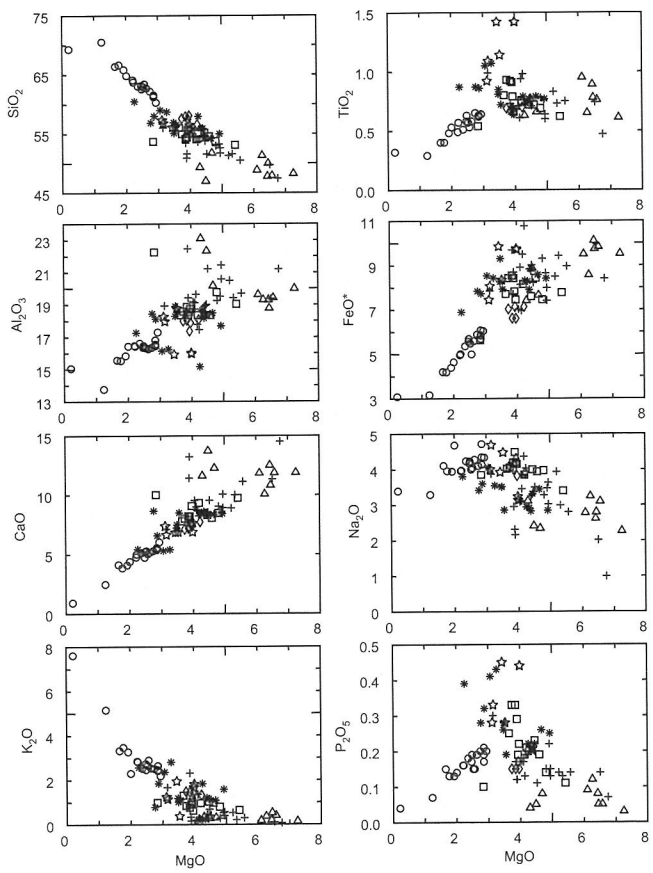

Fig. 7. Oxide variation diagrams of volcanic and plutonic rocks. The symbols are the same as in Fig. 4.

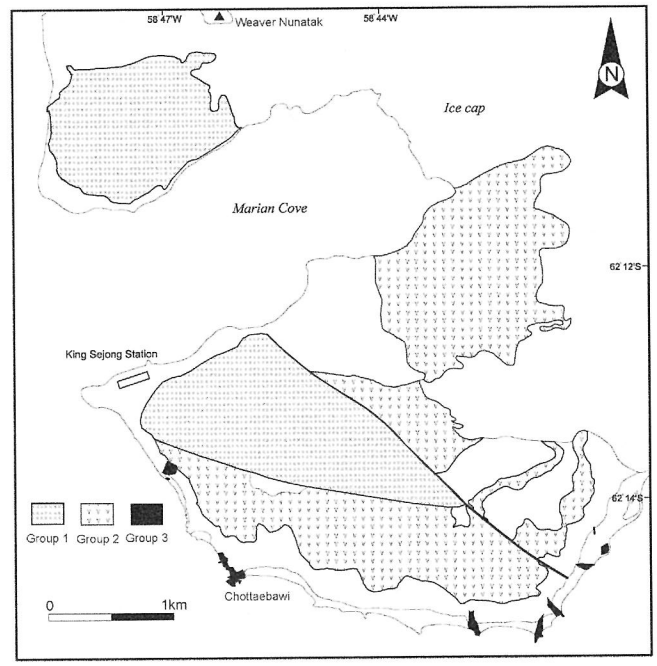

Fig. 8. A map showing regional distribution of three groups of volcanic rocks.

defined differentiation trend in the AFM diagram (Fig. 6) also supports an evolution from single parental magma.

Volcanic rocks are predominated by basaltic andesites with variable Na_2O+K_2O contents, and lack in felsic compositions (Fig. 4). Volcanic rocks with 3 to 5 wt% MgO are highly variable in other oxide contents, particularly in TiO_2, FeO*, Na_2O, and P_2O_5 contents (Fig. 7). This high variability of major element compositions seems to reflect differences in the parental magma composition, though the majority of volcanic rocks broadly show tholeiitic nature. A rather complex differentiation trend in the AFM diagram (Fig. 6) may represent a composite plot of various fractionation trends from different parental magmas.

According to regional distribution and major element chemistry, we divide the volcanic rocks into three groups (Fig. 8). The group 1 rocks are distributed in whole Weaver Peninsula and in the central part of Barton Peninsula bounded by faults trending NW and WNW. They show relatively mafic compositions (basalts to basaltic andesites) with higher MgO, CaO, and Al_2O_3 and lower SiO_2, K_2O, and P_2O_5 contents than the group 2 rocks (Figs. 4 and 7). Some variation trends (e.g., Na_2O vs. MgO and SiO_2 vs. MgO) show apparently different fractionation trends. The group 2 rocks are predominantly distributed in Barton Peninsula, and show intermediate compositions (basaltic andesites to andesites) with significantly higher P_2O_5, K_2O, and SiO_2 and lower MgO, CaO, and Al_2O_3 contents than the group 1 rocks. The group 3 rocks occur as intermediate dikes or plugs along the southern coast of Barton Peninsula. They generally show similar compositions to the group 2 rocks, but significantly higher P_2O_5, Na_2O, and TiO_2 contents than the group 2 rocks at a given MgO content (Fig. 7). These spatial distributions and chemical differences of volcanic rocks may reflect the complexity of parental magma compositions.

4.3. Trace and Rare Earth Element Chemistry

Representative trace element variations of volcanic rocks are shown in Figure 9. Most incompatible elements (except Sr) and high field strength elements (HFSEs) are positively correlated with Zr concentrations. The group 1 rocks show, in general, the lowest concentrations of trace elements and are most depleted. In some diagrams (Y vs. Zr, Th vs. Zr and U vs. Zr), differentiation trends or slopes of group 1 rocks are different from those of the group 2 ones. The group 3 rocks commonly show intermediate compositions between the group 1 and 2 rocks, but they have significantly higher Nb and Hf, and lower Sr and U concentrations than the group 2 rocks at the similar range of Zr concentrations.

In the primitive mantle-normalized trace element variation diagrams (Fig. 10), all the volcanic rocks are relatively enriched in large ion lithophile elements (LILEs) and show prominent negative Nb anomalies. Both features are char-

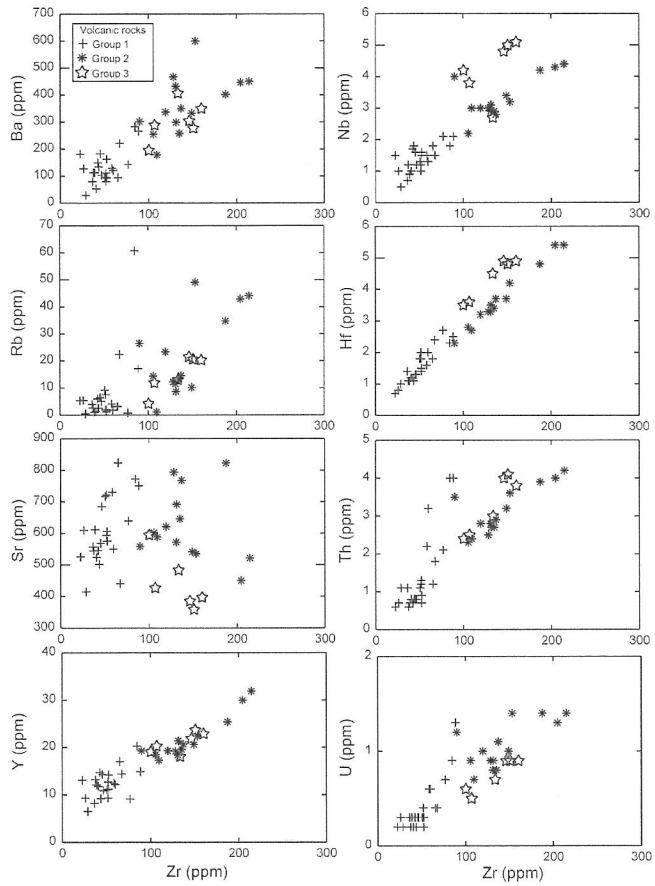

Fig. 9. Variation diagrams of representative trace elements in volcanic rocks.

acteristic for subduction zone magmatism (McCulloch and Gamble, 1991). However, average composition of each group varies. The group 1 rocks have the minimum concentrations of most elements, and the maximum positive anomalies of Pb and Sr. The group 2 and 3 rocks generally show similar trace element patterns, but the former has higher concentrations of LILEs (Rb, Ba and U) and lower concentrations of high field strength elements such as Ti and Yb.

All the rare earth elements (REEs) are positively correlated with Zr concentrations (Fig. 11). The group 1 rocks have relatively depleted nature in both light rare earth element (LREE) and HREE compositions, compared to the group 2 and 3 rocks. The group 2 and 3 rocks show similar compositions of LREEs (La and Nd), but the latter has significantly higher HREE compositions (Gd and Yb). All the volcanic rocks show subparallel REE patterns with LREE enrichment and a continuous decrease toward HREE (Fig. 12). The group 1 rocks have the lowest level of total REEs, and show weakly positive Eu anomalies. Though the group 2 and 3 rocks display similar range of total REEs, the average compositions of HREEs are different (Fig. 12d). The group 2 rocks contain smaller amounts of HREEs, and thus have steeper LREE/HREE ratios.

The differences of trace and rare earth element compositions among three groups may reflect intrinsic geochemical variations in parental magmas. Parental magma of the group 1 rocks should be mostly depleted, whereas that of the group 2 rocks mostly enriched in LILEs and LREEs.

5. DISCUSSION

5.1. Tectonic Setting and Arc Maturity

All the geochemical signatures indicate that the volcanic rocks in the study area were derived from an arc environment. During the Early Tertiary time, King George Island was situated in an active continental margin around the

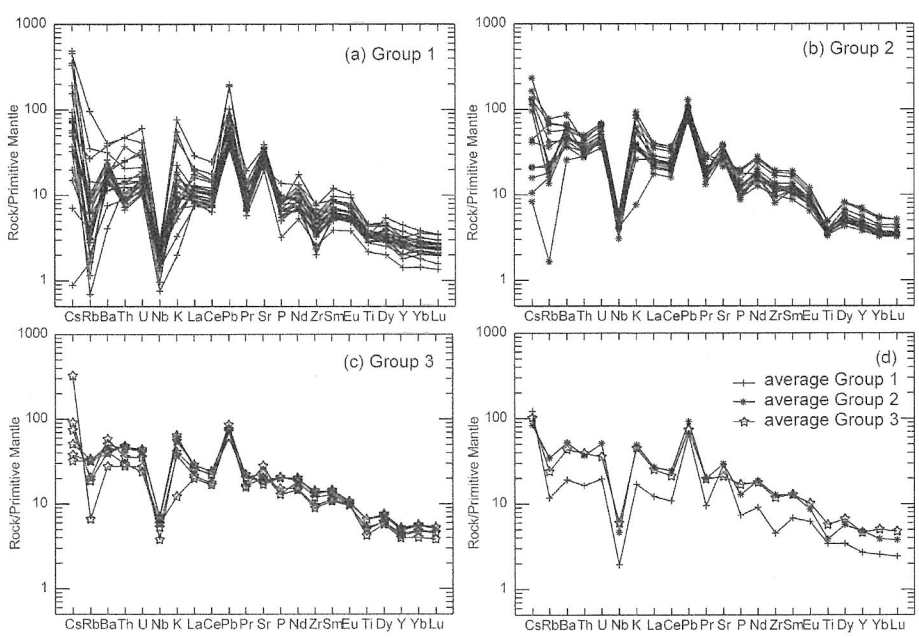

Fig. 10. Primitive mantle-normalized trace element patterns of volcanic rocks. (a) Group 1, (b) group 2, (c) group 3, and (d) average compositions of each group. Compositions of primitive mantle are from Sun and McDonough (1989).

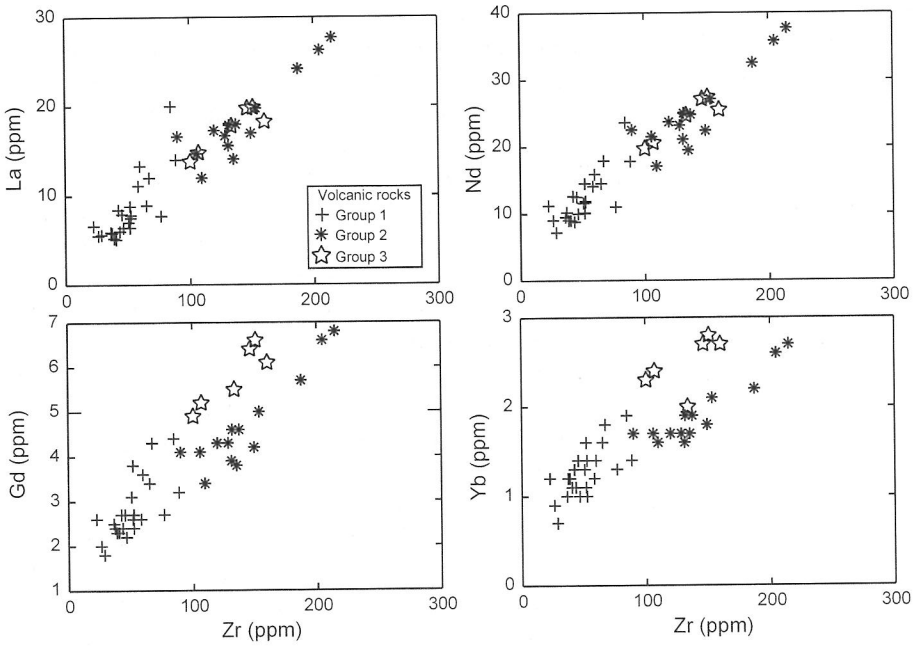

Fig. 11. Variation diagrams of representative rare earth elements in volcanic rocks.

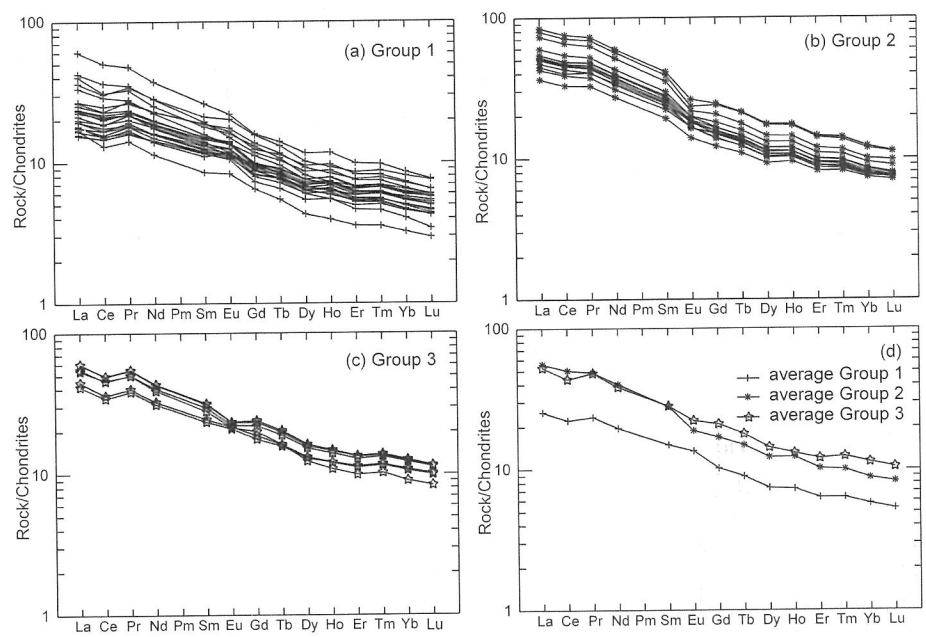

Fig. 12. Chondrite-normalized rare earth element patterns of volcanic rocks. (a) Group 1, (b) group 2, (c) group 3, and (d) average compositions of each group. Chondrite values are from Nakamura (1974).

northern Antarctic Peninsula (Smellie et al., 1984). Previous studies did not pay much attention to the arc maturity of the South Shetland Islands, which is basically related to the development of continental-type crust beneath volcanic arc. According to Miyashiro (1974), major rocks in immature island arcs are commonly basalts and basaltic andesites of the TH series, whereas those in mature ones are andesites and dacites of the TH and CA series. The main volcanic rocks in continental margins are andesites, dacites, and rhyolites of the CA series.

Furthermore, the proportion of CA series rocks among all the volcanic rocks tends to increase with the development of continental-type crust. For example, the representative immature island arcs (Tonga and North Mariana arcs) have less than 10% CA series rocks and a very thin crust (possibly oceanic, <15 km), whereas a well-developed Northeast Japan arc has about 50% CA series rocks, and its crustal thickness is about 30 km. Moreover, a mature island arc tends to have dual volcanic chains along the arc direction (Kushiro, 1987): i.e., TH series on the trench side and CA series on the continental side. The Central Andes, representative continental arc with thick crust, consists primarily of CA series rocks (greater than 95%).

Consequently, the predominance of TH series rocks suggests that the Early Tertiary volcanic activity in KGI occurred in a comparatively immature island arc, though KGI was situated close to the Antarctic Peninsula which is generally considered as a thickened continental margin. The

lack of basement complex in KGI supports this possibility. The dual volcanic chains are not easily recognized in KGI, though Barton (1965) suggested several lines of volcanic centers parallel to the paleo-arc. The volcanic centers (such as Three Brothers Hill, Florence Nunatak, and Czajkowski Needle; Fig. 1) along the line of hypersthene-augite andesites (Barton, 1965) can be considered a continental-side CA series chain, but they are not typically calc-alkaline andesites but transitional basaltic andesites (Lee et al., 1998). Furthermore, one volcanic center (The Tower; Figs. 1 and 3) which is situated further inside the paleo-arc shows typical TH series geochemical nature. It is thus apparent in KGI that the typical dual volcanic chains are ambiguous, and the Plaeocene-Eocene, TH series volcanism occurred in an immature island arc without thickened continental-type crust.

5.2. Geochemical Correlation with Fossilized Volcanic Vents

Volcanic nunataks, such as Three Brothers Hill, Florence Nunatak, and Czajkowski Needle, in the southwestern KGI have been considered as fossilized volcanic vents (Barton, 1965). In addition, Weaver Nunatak and The Tower have been newly recognized as ancient volcanic vents (Lee et al., 1998). These vents comprise subalkaline basaltic andesites to andesites showing low- to medium-K and broadly TH series geochemical nature.

It is remarkable that trace and rare earth element geochemistries are almost identical between basaltic andesites of Weaver Nunatak and the group 1 rocks (Figs. 13a and b), between basaltic andesites of Three Brothers Hill, Florence Nunatak, and Czajkowski Needle and the group 2 (Figs. 13c and d), and between The Tower and the group 3 (Figs. 13e and f). These three pairs of correlated volcanic rocks mostly have negative anomalies for HFSEs such as Nb, Zr, and Ti, together with positive anomalies for LILEs such as Ba, Sr, and Pb (Fig. 13). However, anomaly patterns are different between each pair. The first pair (group 1 and Weaver Nunatak) has the lowest total REE contents and shows strong positive anomalies for Sr and negative anomalies for Zr, indicating the most depleted nature among the three pairs. The other pairs show similar REE patterns, but the second pair (Figs. 13c and d) shows lower levels of HREEs, and thus steeper LREE/HREE ratios (i.e., more incompatible nature). Based on these geochemical correlations, we suggest that each volcanic group in Barton and Weaver peninsulas has formed from different volcanic vents: the group 1 from Weaver Nunatak, and the group 2

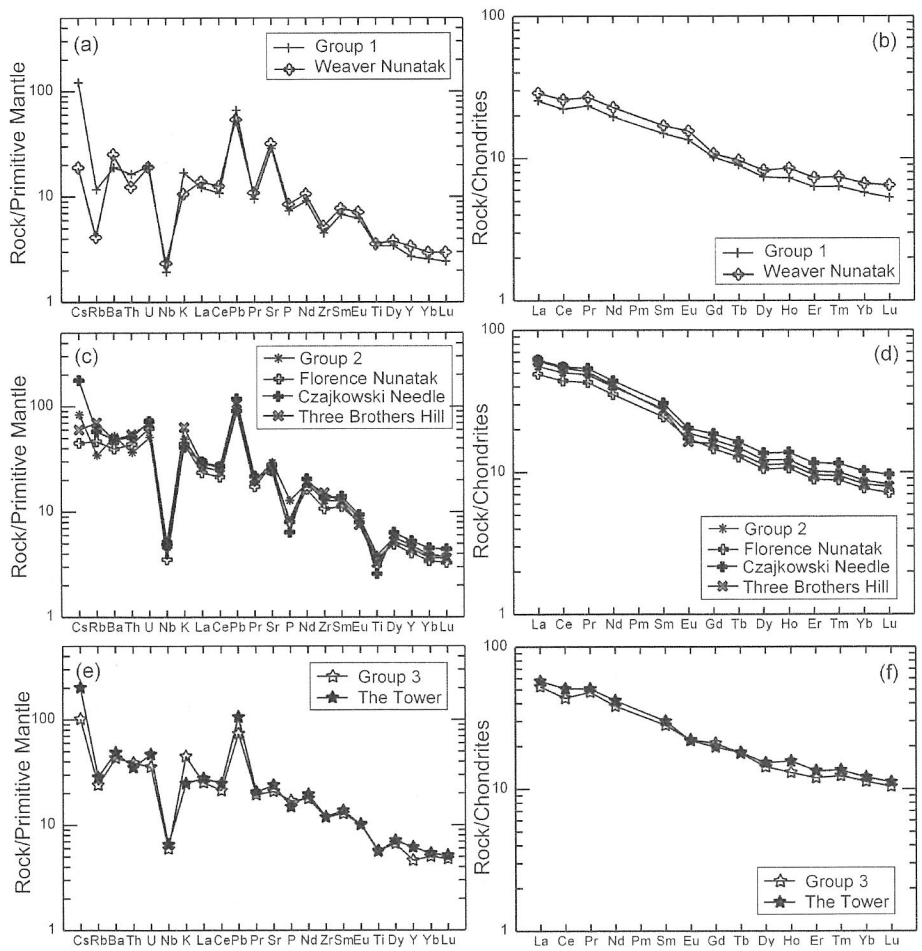

Fig. 13. Geochemical correlation of volcanic rocks with ancient volcanic vents. (a) and (b) Correlation between the group 1 rocks and Weaver Nunatak; (c) and (d) Correlation between the group 2 rocks and Florence Nunatak, Czajkowski Needle, and Three Brothers Hill; (e) and (f) Correlation between the group 3 rocks and The Tower. Average compositions of each group and volcanic vent are plotted for convenience. The data of volcanic vents are from Lee et al. (1998).

from Three Brothers Hill, Florence Nunatak and/or Czajkowski Needle. However, the group 3 rocks are not directly derived from The Tower vent, because the latter is at least 30 km away from Barton Peninsula, and the former commonly occur as dikes or plugs. From the structural analysis, the Polish geologists (Tokarski, 1988; Birkenmajer, 1998) considered a moderate-size plug with 500 m in diameter (the Chottaebawi; the Narebski Point in Polish literatures) in the southern coast of Barton Peninsula as one of big fossilized volcanic vents. The vertical, platy thermal joints are well developed in the eastern part of the plug, and become columnar fan-like ones in its central part. It is thus likely that the group 3 rocks were directly derived from the Chottaebawi plug, or occurred as individual dike swarms. Nevertheless, the geochemical similarity suggests that the group 3 rocks and The Tower are consanguineous.

Finally, it is interesting to note variable occurrences of the group 1 volcanic suite, predominantly forming a dike swarm in Weaver Peninsula but exclusively emplaced as lava flows in Barton Peninsula. The lowermost volcaniclastic member of the study area, Sejong Formation, is only distributed in the lower stratigraphic level of Barton Peninsula, but occurs widely in Weaver Peninsula. This observation indicates that Weaver Peninsula has been uplifted relative to Barton Peninsula. If this is the case, the rocks of Weaver Peninsula would have originally formed at deeper depths than those of Barton Peninsula, but tectonic uplifts could have brought the former to the level comparable to the latter. A large-scale fault is further envisaged between Weaver and Barton peninsulas. It may run parallel to the NE-trending axis of Marian Cove.

6. CONCLUSIONS

1) The Paleocene-Eocene volcanic rocks in Barton and Weaver peninsulas, King George Island, show geochemical properties pertinent to island arc volcanism. The majority of these volcanics were originated from tholeiitic parental magmas. In contrast, major element compositions of plutonic rocks are accounted for by simple fractionation from a calc-alkaline parental magma.

2) Volcanic rocks can be subdivided into three groups based on geochemical characteristics as well as regional distribution. The group 1 rocks are distributed in Weaver Peninsula and in the central part of Barton Peninsula bounded by faults trending NW and NWW. They show relatively mafic compositions (basalts to basaltic andesites) with higher MgO, CaO, and Al_2O_3 and lower SiO_2, K_2O, and P_2O_5 contents than the group 2 rocks. The group 2 rocks are widely distributed in Barton Peninsula, and show intermediate compositions (basaltic andesites to andesites) with significantly higher P_2O_5, K_2O, and SiO_2 and lower MgO, CaO, and Al_2O_3 contents than the group 1 rocks. The group 3 rocks occur as intermediate dikes or plugs along the southern coast of Barton Peninsula. They generally show similar compositions to the group 2 rocks, but contain significantly higher P_2O_5, Na_2O, and TiO_2 contents than the group 2 rocks.

3) The group 1 rocks have the lowest level of total REEs, and show weakly positive Eu anomalies. Although the group 2 and 3 contain similar amounts of total REEs, the group 2 rocks are lower in HREE contents, and thus have steeper LREE/HREE ratios. The parental magma of the group 1 is most depleted, whereas that of the group 2 most enriched in LILEs and LREEs.

4) Predominance of tholeiite series rocks, general absence of basement complex, and difficulty of identifying dual volcanic chains suggest that the Early Tertiary volcanism in King George Island occurred in an immature island arc without thickened continental-type crust.

5) Based on the geochemical correlations between volcanic rocks and fossilized volcanic vents, each volcanic group in Barton and Weaver peninsulas can be correlated with its possible vent: the group 1 with Weaver Nunatak, and the group 2 with Three Brothers Hill, Florence Nunatak and/or Czajkowski Needle. However, the group 3 seems to have been derived from the Chottaebawi plug (the Narebski Point), or occurred as individual dike swarms, because The Tower vent, chemically identical to the group 3, is far away from Barton Peninsula.

ACKNOWLEDGMENTS: This study was supported by KORDI (Korea Ocean Research and Development Institute) grant PP03103. We would like to thank Prof. M. Cho of Seoul National University, Dr. H.Y. Lee of KIGAM, and Dr. S.B. Kim of KORDI for constructive comments that improved the manuscript.

REFERENCES

Ashcroft, W.A., 1972, Crustal Structure of the South Shetland Islands and Bransfield Strait. British Antarctic Survey Scientific Report 66, 43 p.

Barker, P.F. and Griffiths, D.H., 1972, The evolution of the Scotia Ridge and Scotia Sea. Philosophical Transactions of the Royal Society of London, Series A, 271, p. 151–183.

Barton, C.M., 1965, The Geology of the South Shetland Islands: III. The Stratigraphy of King George Island. British Antarctic Survey Scientific Report 44, 33 p.

Birkenmajer, K., 1983, Late Cenozoic phases of block-faulting on King George Island (South Shetland Islands, West Antarctica). Bulletin of the Polish Academy of Sciences (Earth Sciences), 30, 21–32.

Birkenmajer, K., 1998, Geological structure of Barton Peninsula and Weaver Peninsula, Maxwell Bay, King George Island (South Shetland Islands, West Antarctica). Bulletin of the Polish Academy of Sciences (Earth Sciences), 46, 191–209.

Birkenmajer, K., Guterch, A., Grad, M., Janik, T. and Perchuc, E., 1990, Lithospheric transect Antarctic Peninsula - South Shetland Islands, West Antarctica. Polish Polar Research, 11, 241–258.

Chun, H.Y., Chang, S.K. and Lee, J.I., 1994, Biostratigraphic study on the plant fossils from the Barton Peninsula and adjacent area.

Journal of the Paleontological Society of Korea, 10, 69–84. (in Korean)

Davies, R.E.S., 1982, The geology of the Marian Cove Area, King George Island and Tertiary age for its supposed Jurassic rocks. British Antarctic Survey Bulletin, 51, 151–165.

Hur, S.D., Lee, J.I., Hwang, J. and Choe, M.Y., 2001, K-Ar age and geochemistry of hydrothermal alteration in the Barton Peninsula, King George Island, Antarctica. Ocean and Polar Research, 23, 11–21. (in Korean)

Irvine, T.N. and Baragar, W.R.A., 1971, A guide to the chemical classification of the common volcanic rocks. Canadian Journal of Earth Sciences, 8, 523–548.

IUGS (International Union of Geological Sciences), 1973, Classification and nomenclature of plutonic rocks: recommendations. Geological News Letters, 2, 110–127.

Jwa, Y.-J. and Lee, J.I., 1992, Geochemistry of the volcanic rocks from the Fildes Peninsula, King George Island, Antarctica. Journal of the Korean Earth Science Society, 13, 200–211. (in Korean)

Jwa, Y.-J., Park, B.-K. and Kim, Y., 1992, Geochronology and geochemistry of the igneous rocks from Barton and Weaver peninsulas, King George Island: A review. In: Yoshida, Y., Kaminuma, K. and Shiraishi, K. (eds.), Recent Progress in Antarctic Earth Science. Terra Scientific Publishing Company, Tokyo, p. 439–442.

Kim, H., Lee, J.I., Choe, M.Y., Cho, M., Zheng, X., Sang, H. and Qin, J., 2000, Geochronologic evidence for Early Cretaceous volcanic activity on Barton Peninsula, King George Island, Antarctica. Polar Research, 19, 251–260.

Kim, H., Cho, M. and Lee, J.I., 2002, Thermal metamorphism of volcanic rocks on Barton Peninsula, King George Island, Antarctica. Geosciences Journal, 6, 303–317.

Kushiro, I., 1987, A petrological model of the mantle wedge and lower crust in the Japanese islands arcs. In: Mysen, B.O. (ed.) Magmatic Process: Physicochemical Principles. Geochemical Society, Special Publication, 1, p. 165–181.

Lee, J.I., 1994, A Study on the Development of Quantitative Analytical Program of the Granitic Rocks Using an X-Ray Fluorescence. Report BSPE 00431-671-7, Korea Ocean Research and Development Institute, Ansan, 43 p. (in Korean)

Lee, J.I., Hwang, J., Kim, H., Kang, C.Y., Lee, M.J. and Nagao, K., 1996, Subvolcanic zoned granitic pluton in the Barton and Weaver peninsulas, King George Island, Antarctica. Proceedings of the NIPR Symposium on Antarctic Geosciences, 9, p. 76–90.

Lee, J.I., Choe, M.Y., Kim, H. and Hur, S.D., 1998, Petrography and geochemistry of volcanic nunataks in the southwestern King George Island, Antarctica. Report BSPP 98001-04-1149-7, Korea Ocean Research and Development Institute, Aasan, p. 417–450. (in Korean)

Lee, J.I., Hur, S.D., Yoo, C.M., Yeo, J.P., Kim, H., Hwang, J., Choe, M.Y., Nam, S.H., Kim, Y., Park, B.-K., Zheng, X. and Lopez-Martinez, J., 2002, Geological Map of Barton and Weaver Peninsulas, King George Island, Antarctica. Korea Ocean Research and Development Institute, Ansan, 30 p.

Le Maitre, R.W., Bateman, P., Dudek, A., Keller, J., Lameyre Le Bas, M.J., Sabine, P.A., Schmid, R., Sorensen, H., Streckeisen, A., Woolley, A.R. and Zanettin, B., 1989, A Classification of Igneous Rocks and Glossary of Terms. Blackwell Scientific Publications, London, 193 p.

McCulloch, M.T. and Gamble, J.A., 1991, Geochemical and geodynamical constraints on subduction zone magmatism. Earth and Planetary Science Letters, 102, 358–374.

Miyashiro, A., 1974, Volcanic rock series in island arcs and active continental margins. American Journal of Science, 274, 321–355.

Nakamura, N., 1974, Determination of REE, Ba, Fe, Mg, Na and K in carbonaceous and ordinary chondrites. Geochimica et Cosmochimica Acta, 38, 757–775.

Osborn, E.F., 1962, Reaction series for subalkaline igneous rocks based on different oxygen pressure conditions. American Mineralogist, 47, 211–226.

Pankhurst, R.J. and Smellie, J.L., 1983, K-Ar geochronology of the South Shetland Islands, Lesser Antarctica: Apparent lateral migration of Jurassic to Quaternary island arc volcanism. Earth and Planetary Science Letters, 66, 214–222.

Park, B.-K., 1989, Potassium-argon radiometric ages of volcanic and plutonic rocks from the Barton Peninsula, King George Island, Antarctica. Journal of the Geological Society of Korea, 25, 495–497.

Sakuyama, M., 1979, Lateral variation of H_2O contents in Quaternary magmas of northeastern Japan. Earth and Planetary Science Letters, 43, 103–111.

Smellie, J.L., Pankhurst, R.J., Thomson, M.R.A. and Davies, R.E.S., 1984, The Geology of the South Shetland Islands: VI. Stratigraphy, Geochemistry and Evolution. British Antarctic Survey Scientific Report 87, 85 p.

Sun, S.-S. and McDonough, W.F., 1989, Chemical and isotopic systematics of oceanic basalts: implications for mantle composition and processes. In: Saunders, A.D. and Norry, M.J. (eds.), Magmatism in the Ocean Basins. Geological Society Special Publication, 42, p. 315–345.

Tatsumi, Y. and Eggins, S., 1995, Subduction Zone Magmatism. Blackwell Science, Cambridge, 211 p.

Tokarski, A.K., 1988, Structural analysis of Barton Peninsula (King George Island, West Antarctica): an example of volcanic arc tectonics. Studia Geologica Polonica, 95, 53–63.

Willan, R.C.R. and Armstrong, D.C., 2002, Successive geothermal, volcanic-hydrothermal and contact-metasomatic events in Cenozoic volcanic-arc basalts, South Shetland Islands, Antarctica. Geological Magazine, 139, 209–231.

Yoo, C.M., Choe, M.Y., Jo, H.R., Kim, Y. and Kim, K.H., 2001, Volcaniclastic sedimentation of the Sejong Formation (Late Paleocene-Eocene), Barton Peninsula, King George Island, Antarctica. Ocean and Polar Research, 23, 97–107.

Manuscript received June 3, 2003
Manuscript accepted February 10, 2004